

Supporting Information

Colorimetric CRISPR Biosensor: A Case Study with *Salmonella Typhi*.

Ana Pascual-Garrigos¹, Beatriz Lozano-Torres¹, Akashaditya Das², Jennifer Molloy^{1*}

¹ Department of Chemical Engineering and Biotechnology, University of Cambridge, Cambridge CB3 0AS

² Department of Chemical Engineering, Imperial College London, London SW7 2AZ, United Kingdom.

CRISPR-Cas12, colorimetric, b-galactosidase, DNA, biosensor

Table S1. Colorimetric approaches coupled with CRISPR-Cas12.

Method	Model of action	Strengths	Weakness
DNA-conjugated nanoparticle dispersion ¹⁻³	CRISPR cleavage breaks the DNA sequences responsible for nanoparticle aggregation resulting in a color change as nanoparticles disperse.	One-step reaction	Biofluids can cause aggregation leading to false negatives Color change from red to purple may not be obvious Linear signal amplification
DNA-conjugated nanoparticle dispersion and separation ^{4,5}	CRISPR cleavage breaks the DNA sequences responsible for nanoparticle aggregation. The aggregated sample can be separated using a centrifuge or a magnet, if magnetic beads are used.	Clear color change	Two-step reaction Biofluids can cause aggregation leading to false negatives Counterintuitive color change with red being a negative result and colorless being a positive result. Linear signal amplification
3,3'-diethylthiadicarbocyanine iodide (DISC2(5)) ⁶	DISC ₂ (5) is a colorimetric molecule that is purple in its free form. It can specifically bind consecutive thymidine adenine pairs in dsDNA which causes dimerization of the agent and produces a blue color. In the presence of active Cas12, the dsDNA can be degraded and produce a color change from blue to purple.	No labels needed on the oligonucleotides used, reducing the cost One-step reaction	Color change from blue to purple may not be obvious Linear signal amplification
Platinum nanoparticles ⁷	Platinum nanoparticles tethered to magnetic beads by single-stranded DNA are released upon cleavage and travel to a hydrogen peroxide chamber inside a volumetric bar-chart chip. This results in the production of	Quantitative Shows detection of single nucleotide variations	Costly manufacture to the chip Linear signal amplification

	oxygen moving an ink droplet in the device.		
G-Quadruplex DNzyme ⁸	Guanine quadruplexes are complex DNA structures known for their peroxidase-mimicking activity. When intact, they produce color in the presence of ABTS, but if disrupted this activity ceases.	No labels needed on the oligonucleotides used, reducing the cost. One-step reaction Clear color difference	Counterintuitive color change with green being a negative result and colorless being a positive result. Linear signal amplification
Fluorophore-quencher probe ⁹	Fluorophore-quencher DNA probe as is usually used in fluorescent assays but using a fluorophore which is visible to the naked eye such as ROX. ROX produces a color change from blue to red.	One-step reaction Clear color change Shown to work with heat from a handwarmer	Photosensitive Limitation on how many fluorophores are visible to the naked eye without blue light being necessary Linear signal amplification
Urease-oligonucleotide conjugation ¹⁰	Urease enzymes are tethered to magnetic beads by ssDNA and immobilized. When the enzymes are released by activated Cas12, they are separated and mixed with urea and phenol red. Urea is hydrolyzed and the pH increase produced by the reaction changes the color of phenol red from yellow to red.	Clear color change Exponential signal increase	Urea interferant excluding the use of urine samples. Biofluids could change the pH, interfering with the assay. Two-step reaction
HRP-oligonucleotide conjugation ^{5,11–14}	An oligo conjugated to HRP and immobilized on a magnetic bead is cleaved by active Cas12. Upon release, the HRP is isolated and mixed with TMB and hydrogen peroxide resulting in the oxidation of the TMB causing an intense blue color.	Clear color change Exponential signal increase	Protein difficult to produce in <i>E. coli</i> . Two-step reaction
LacZ-oligonucleotide conjugation (this work)	A DNA-β-galactosidase conjugate was produced and immobilized to a surface. When cleaved in the presence of target-activated CRISPR-Cas12 the colorimetric enzyme is released, and the supernatant transferred to an environment containing X-Gal producing an intense blue color.	Distinct color change. Exponential signal increase Enzyme easy to produce in <i>E. coli</i> . Can be lyophilized.	Two-step reaction

Table S2. DNA sequences of the modified oligonucleotides used for conjugation with LacZ.

DNA ₂₀	/5AmMC12/TCAACGACTGACTGAGCTCT
BioDNA ₂₀	/5AmMC12/TCAACGACTGACTGAGCTCT/3Bio/
BioDNA ₄₀	/5AmMC12/TCAACGACTGACTGAGCTCTGATCGAATTCTGACACTACG/3Bio/

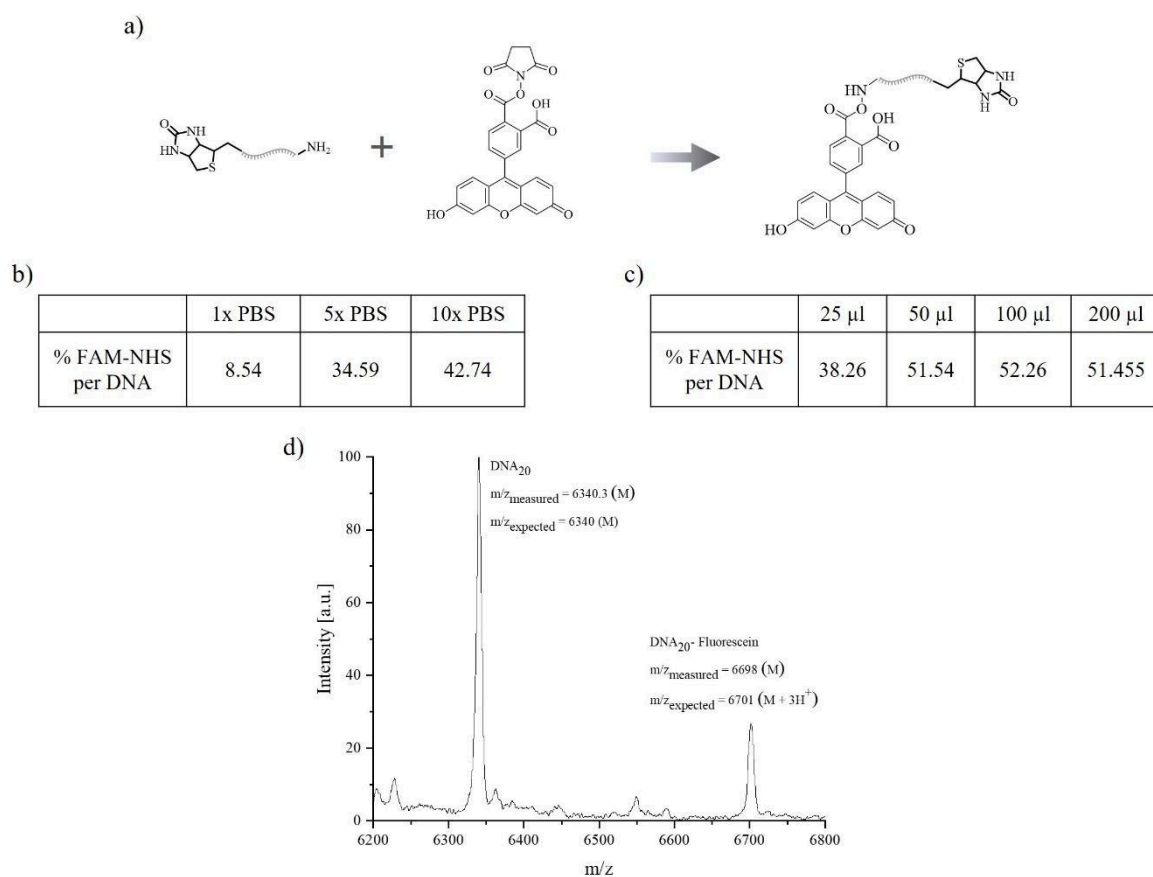


Figure S1. Amineylated DNA-NHS ester reaction optimization. a) Scheme of the reaction to obtain fluorescein conjugated to DNA [illustration created with ChemDraw]. b) PBS concentration titration in 100 μ l volume at pH 8.4 with 10 nmol of amineylated and 100 nmol FAM-NHS. c) Volume titration in 10x PBS at pH 8.4 with 10 nmol of amineylated and 100 nmol FAM-NHS. d) Mass spectrometry of the reaction in part b.

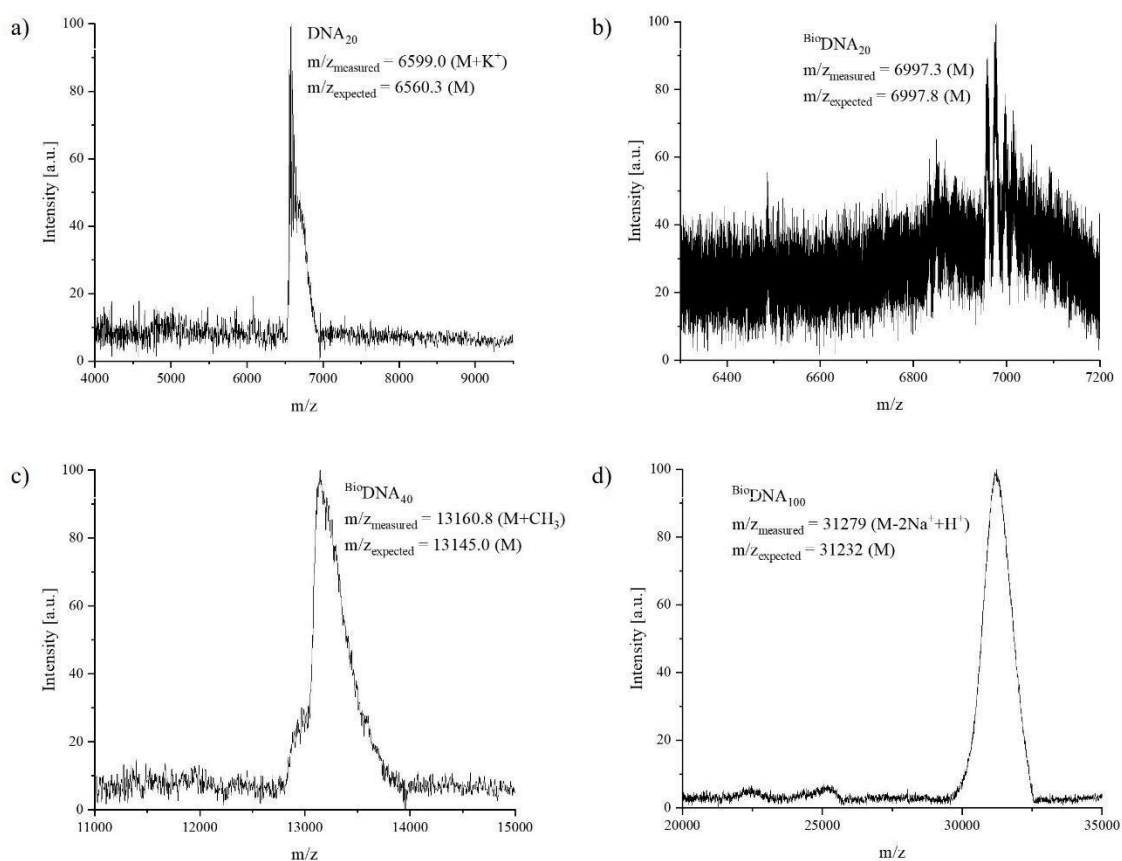


Figure S2. MALDI-TOFs of DNA-SMCC samples. a) 20 bp 5' aminylated DNA. b) 20 bp 5' aminylated and 3' biotinylated DNA. c) 40 bp 5' aminylated and 3' biotinylated DNA. d) 100 bp 5' aminylated and 3' biotinylated DNA.

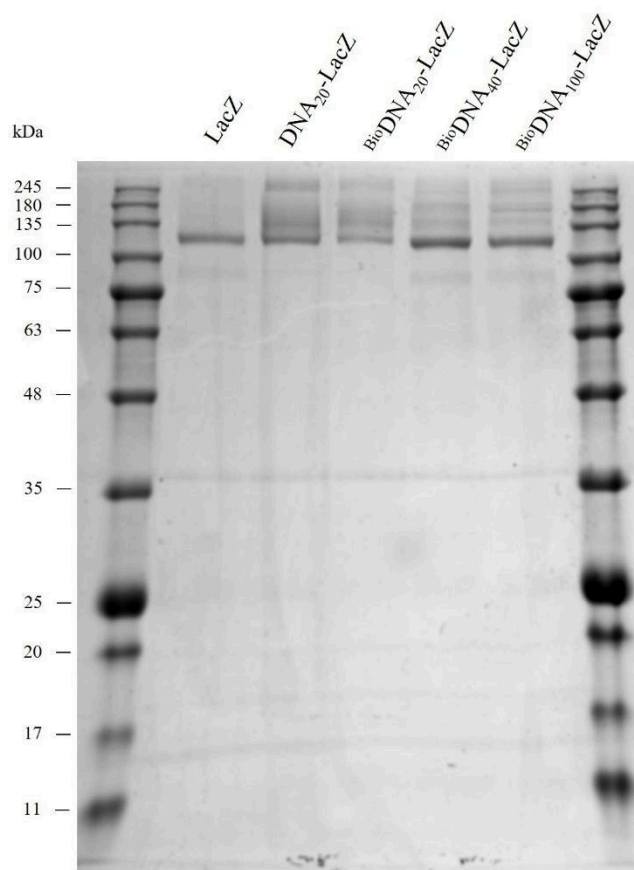


Figure S3. SDS-PAGE of LacZ at ~118 kDa vs. DNA-LacZ conjugates at the same and higher masses.

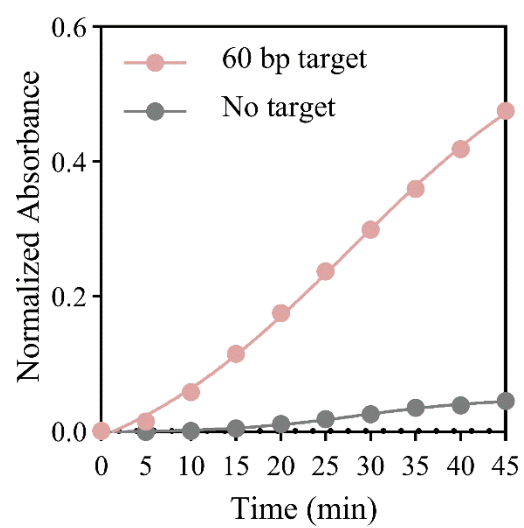


Figure S4. Normalized absorbance kinetics after CRISPR conjugate cleavage with 7.5 nM 60 bp target vs. no target.

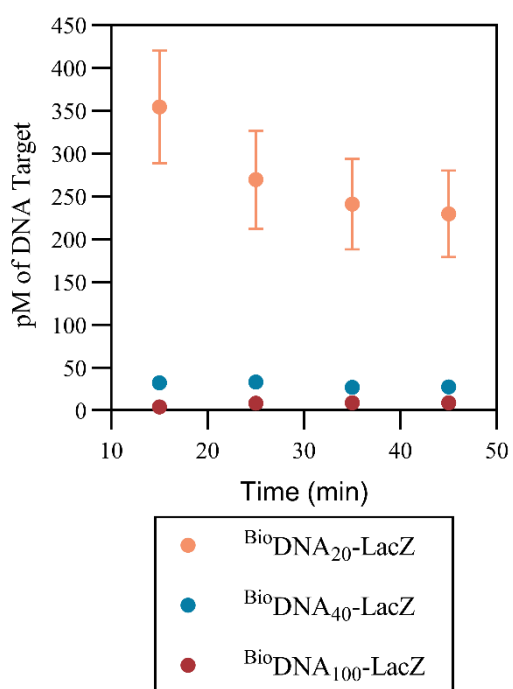


Figure S5. Calculated limits of detection of each conjugate based on the absorbance obtained over time.

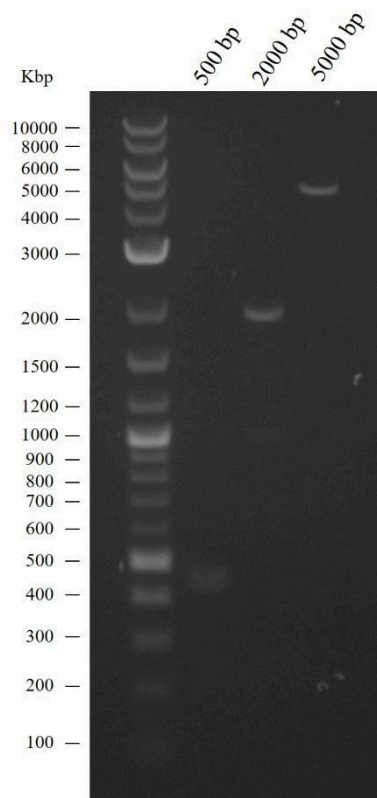


Figure S6. Gel electrophoresis of 500, 2000 and 5000 bp *S. Typhi* target amplicons.

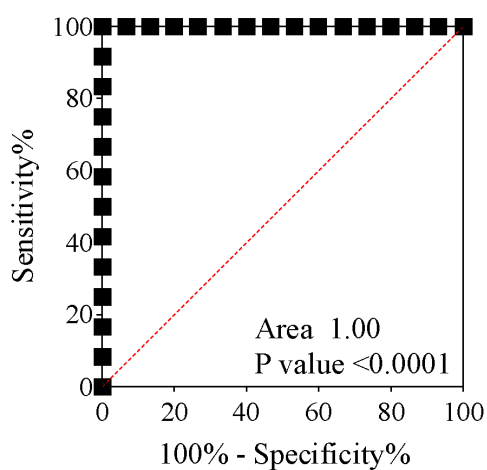


Figure S7. ROC curve based on the absorbances obtained after 45 minutes of incubation in the presence of target amplicons vs. off-target samples.

For LacZ, it was clear that an additive was necessary since all activity was lost without one after freeze drying, while most additives tested allowed it to maintain its activity. It is important to note, that although LacZ remained active after freeze drying, all additives had some inhibitory effect. Cas12 could maintain some activity without an additive but was also inhibited by most of the compounds tested. The exceptions to this were D-Glucose, Sucrose and D-(+)-Trehalose dihydrate with trehalose being the highest performing one, and therefore, selected for the full system.

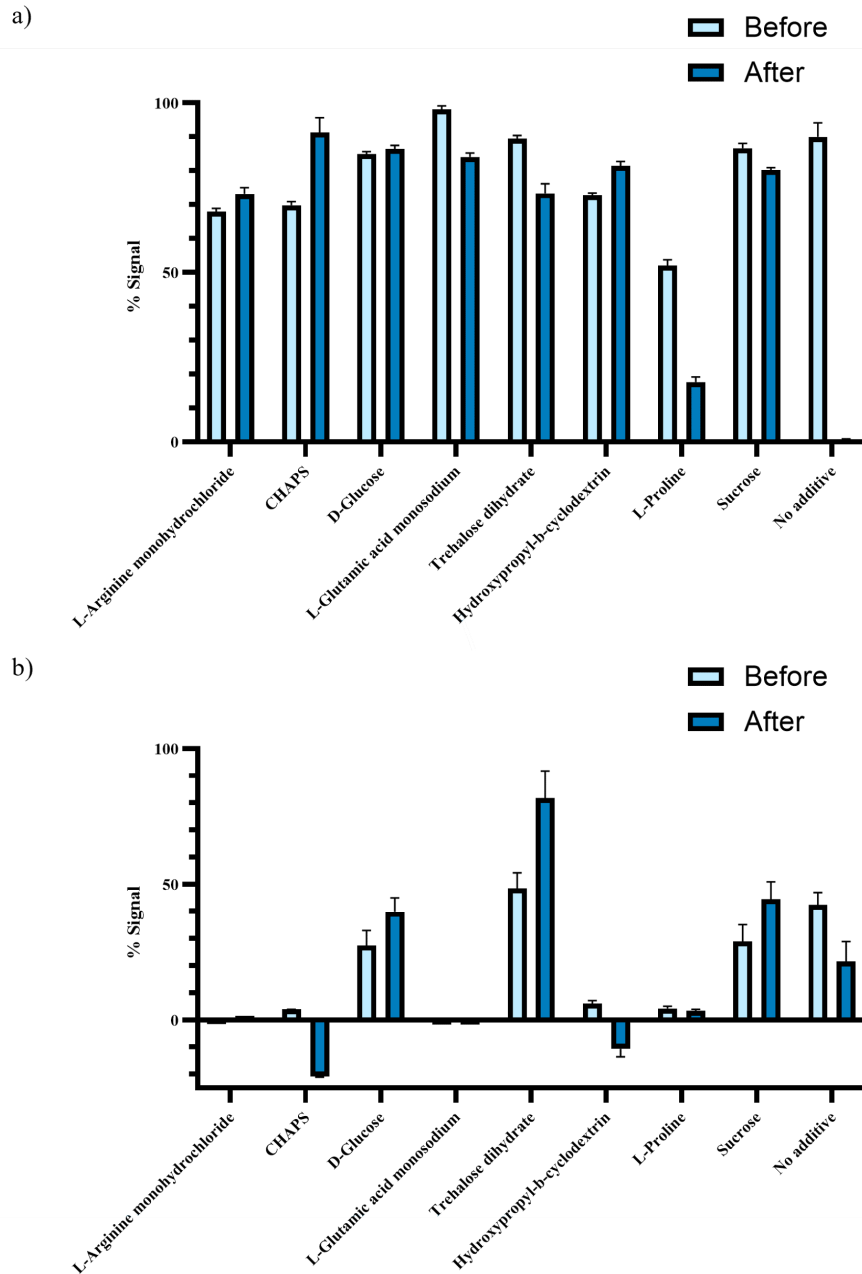


Figure S8. Additive effect on enzyme activity before and after lyophilization. a) 10% w/v additives mixed with 0.8 μ g LacZ. Enzyme rehydrated to the original volume with water and mixed with X-Gal at a final solution of 2.5 mg/ml. Absorbance measured after 20 minutes of incubation at 37 $^{\circ}$ C, subtracted by the signal at time zero and divided by the highest absorbance value across all conditions. b) 10% w/v additives mixed with 75 nM LbaCas12a, 95 nM gRNA and 1x CutsmartT. Components rehydrated to the original volume with water and mixed with 10 nM 60 bp synthetic DNA target and 0.5 μ M FQ reporter. Fluorescence measured after 20 minutes of incubation at 37 $^{\circ}$ C, subtracted by the signal at time zero and divided by the highest fluorescence value across all conditions.

References

- (1) Zhang, W. S.; Pan, J.; Li, F.; Zhu, M.; Xu, M.; Zhu, H.; Yu, Y.; Su, G. Reverse Transcription Recombinase Polymerase Amplification Coupled with CRISPR-Cas12a for Facile and Highly Sensitive

- Colorimetric SARS-CoV-2 Detection. *Anal. Chem.* **2021**, *93* (8), 4126–4133. <https://doi.org/10.1021/acs.analchem.1c00013>.
- (2) Wang, W.; Liu, J.; Li, X.; Lin, C.; Wang, X.; Liu, J.; Ling, L.; Wang, J. CRISPR/Cas12a-Based Biosensor for Colorimetric Detection of Serum Prostate-Specific Antigen by Taking Nonenzymatic and Isothermal Amplification. *Sensors and Actuators B: Chemical* **2022**, *354*, 131228. <https://doi.org/10.1016/j.snb.2021.131228>.
 - (3) Zhang, Y.; Chen, M.; Liu, C.; Chen, J.; Luo, X.; Xue, Y.; Liang, Q.; Zhou, L.; Tao, Y.; Li, M.; Wang, D.; Zhou, J.; Wang, J. Sensitive and Rapid On-Site Detection of SARS-CoV-2 Using a Gold Nanoparticle-Based High-Throughput Platform Coupled with CRISPR/Cas12-Assisted RT-LAMP. *Sensors and Actuators B: Chemical* **2021**, *345*, 130411. <https://doi.org/10.1016/j.snb.2021.130411>.
 - (4) Cao, Y.; Wu, J.; Pang, B.; Zhang, H.; Le, X. C. CRISPR/Cas12a-Mediated Gold Nanoparticle Aggregation for Colorimetric Detection of SARS-CoV-2. *Chem. Commun.* **2021**, *57* (56), 6871–6874. <https://doi.org/10.1039/D1CC02546E>.
 - (5) Hu, M.; Yuan, C.; Tian, T.; Wang, X.; Sun, J.; Xiong, E.; Zhou, X. Single-Step, Salt-Aging-Free, and Thiol-Free Freezing Construction of AuNP-Based Bioprobes for Advancing CRISPR-Based Diagnostics. *J. Am. Chem. Soc.* **2020**, *142* (16), 7506–7513. <https://doi.org/10.1021/jacs.0c00217>.
 - (6) Kim, H.; Jang, H.; Song, J.; Lee, S. M.; Lee, S.; Kwon, H.-J.; Kim, S.; Kang, T.; Park, H. G. A CRISPR/Cas12 Trans-Cleavage Reporter Enabling Label-Free Colorimetric Detection of SARS-CoV-2 and Its Variants. *Biosensors and Bioelectronics* **2024**, *251*, 116102. <https://doi.org/10.1016/j.bios.2024.116102>.
 - (7) Shao, N.; Han, X.; Song, Y.; Zhang, P.; Qin, L. CRISPR-Cas12a Coupled with Platinum Nanoreporter for Visual Quantification of SNVs on a Volumetric Bar-Chart Chip. *Anal. Chem.* **2019**, *91* (19), 12384–12391. <https://doi.org/10.1021/acs.analchem.9b02925>.
 - (8) Chen, X.; Wang, L.; He, F.; Chen, G.; Bai, L.; He, K.; Zhang, F.; Xu, X. Label-Free Colorimetric Method for Detection of *Vibrio Parahaemolyticus* by Trimming the G-Quadruplex DNAzyme with CRISPR/Cas12a. *Anal. Chem.* **2021**, *93* (42), 14300–14306. <https://doi.org/10.1021/acs.analchem.1c03468>.
 - (9) Xie, S.; Tao, D.; Fu, Y.; Xu, B.; Tang, Y.; Steinaa, L.; Hemmink, J. D.; Pan, W.; Huang, X.; Nie, X.; Zhao, C.; Ruan, J.; Zhang, Y.; Han, J.; Fu, L.; Ma, Y.; Li, X.; Liu, X.; Zhao, S. Rapid Visual CRISPR Assay: A Naked-Eye Colorimetric Detection Method for Nucleic Acids Based on CRISPR/Cas12a and a Convolutional Neural Network. *ACS Synth. Biol.* **2022**, *11* (1), 383–396. <https://doi.org/10.1021/acssynbio.1c00474>.
 - (10) Ki, J.; Na, H.-K.; Yoon, S. W.; Le, V. P.; Lee, T. G.; Lim, E.-K. CRISPR/Cas-Assisted Colorimetric Biosensor for Point-of-Use Testing for African Swine Fever Virus. *ACS Sens* **2022**, *7* (12), 3940–3946. <https://doi.org/10.1021/acssensors.2c02007>.
 - (11) Zheng, L.; Jiang, Y.; Huang, F.; Wu, Q.; Lou, Y. A Colorimetric, Photothermal, and Fluorescent Triple-Mode CRISPR/Cas Biosensor for Drug-Resistance Bacteria Detection. *Journal of Nanobiotechnology* **2023**, *21* (1), 493. <https://doi.org/10.1186/s12951-023-02262-x>.
 - (12) Mu, X.; Li, J.; Xiao, S.; Xu, J.; Huang, Y.; Zhao, S.; Tian, J. Peroxidase-Mimicking DNA-Ag/Pt Nanoclusters Mediated Visual Biosensor for CEA Detection Based on Rolling Circle Amplification and CRISPR/Cas 12a. *Sensors and Actuators B: Chemical* **2023**, *375*, 132870. <https://doi.org/10.1016/j.snb.2022.132870>.
 - (13) Park, D. H.; Haizan, I.; Ahn, M. J.; Choi, M. Y.; Kim, M. J.; Choi, J.-H. One-Pot CRISPR-Cas12a-Based Viral DNA Detection via HRP-Enriched Extended SsDNA-Modified Au@Fe₃O₄ Nanoparticles. *Biosensors* **2024**, *14* (1), 26. <https://doi.org/10.3390/bios14010026>.
 - (14) Cao, H.; Mao, K.; Yang, J.; Wu, Q.; Hu, J.; Zhang, H. High-Throughput MPAD with Cascade Signal Amplification through Dual Enzymes for ArsM in Paddy Soil. *Anal. Chem.* **2024**. <https://doi.org/10.1021/acs.analchem.3c05958>.